workshop on placenta derived stem cells. *Stem Cells*, 2008, **26**, 300–311.
17. Sheppard, D. N. and Welsh, M. J., Structure and function of the CFTR chloride channel. *Physiol. Rev.*, 1999, **79**, 23–45.
18. Toshio, M., Amnion-derived stem cells: in quest of clinical applications. *Stem Cell Res. Ther.*, 2011, **2**(3), 25.
19. Li, H., Niederkorn, J. Y., Neelam, S., Mayhew, E., Word, R. A., McCulley, J. P. and Alizadeh, H., Immunosuppressive factors secreted by human amniotic epithelial cells. *Invest. Ophthalmol. Vis. Sci.*, 2005, **46**, 900–907.
20. Lindvall, O. and Kokaia, Z., Recovery and rehabilitation in stroke: stem cells. *Stroke*, 2004, **35**, 2691–2694.
21. Meisel, C. and Meisel, A., Suppressing immunosuppression after stroke. *N. Engl. J. Med.*, 2011, **365**, 2134–2136.
22. Moodley, Y. *et al.*, Human amnion epithelial cell transplantation abrogates lung fibrosis and augments repair. *Am. J. Respir. Crit. Care Med.*, 2010, **182**, 643–651.
23. Murphy, S., Lim, R., Dickinson, H., Acharya, R., Rosli, S., Jenkin, G. and Wallace, E., Human amnion epithelial cells prevent bleomycin-induced lung injury and preserve lung function. *Cell Transplant.*, 2011, **20**, 909–923.
24. Broughton, B. R., Lim, R., Arumugam, T. V., Drummond, G. R., Wallace, E. M. and Sobey, C. G., Post-stroke inflammation and the potential efficacy of novel stem cell therapies: focus on amnion epithelial cells. *Front Cell Neurosci.*, 2013, **6**, 66.
25. Meng, X. T., Chen, D., Dong, Z. Y. and Liu, J. M., Enhanced neural differentiation of neural stem cells and neurite growth by amniotic epithelial cell co-culture. *Cell Biol. Int.*, 2007, **31**, 691–698.
26. Venkatachalam, S., Palaniappan, T., Jayapal, P. K., Neelamegan, S., Rajan, S. S. and Muthiah, V. P., Novel neurotrophic factor secreted by amniotic epithelial cells. *Biocell*, 2009, **33**, 81–89.
27. Chen, Y. T. *et al.*, Human amniotic epithelial cells as novel feeder layers for promoting *ex vivo* expansion of limbal epithelial progenitor cells. *Stem Cells*, 2007, **25**, 1995–2005.
28. Kinoshita, S., Adachi, W., Sotozono, C., Nishida, K., Yokoi, N., Quantock, A. J. and Okubo, K., Characteristics of the human ocular surface epithelium. *Prog. Retin. Eye Res.*, 2001, **20**, 639–673.
29. Ghoubay-Benallaoua, D., Basli, E., Goldschmidt, P., Pecha, F., Chaumeil, C., Laroche, L. and Borderie, V., Human epithelial cell cultures from superficial limbal explants. *Mol. Vis.*, 2011, **17**, 341–354.

ACKNOWLEDGEMENTS. This study was supported by the Natural Science Foundation of Heilongjiang Province, China (grant number D200956), partially funded by the National Natural Science Foundation (NSFC: 30970749).

Received 11 October 2014; revised accepted 15 November 2015

doi: 10.18520/cs/v110/i9/1839-1844

Delineation of Trap and subtrappean Mesozoic sediments in Saurashtra peninsula, India

A. S. N. Murty[1,*], Kalachand Sain[2], V. Sridhar[2], A. S. S. S. R. S. Prasad[2] and S. Raju[2]

[1]No. 19-104/4, Kalyanapuri, Uppal, Hyderabad 500 039, India
[2]CSIR-National Geophysical Research Institute, Uppal Road, Hyderabad 500 007, India

Mapping of sediments beneath volcanic Traps is a highly challenging task. Here we report on the analysis of wide-angle seismic data from Trap-covered Saurashtra peninsula to address this problem. Travel-time modelling of mainly seismic refraction and some reflection phases yields basement configuration, trap and subtrappean sediment thicknesses along the Jodia–Ansador (NW–SE) profile in Saurashtra peninsula. Travel-time skip and amplitude decay in seismic refraction data indicate the presence of low-velocity sediments beneath the Traps. The result reveals two layers with Deccan Traps (4.85–5.0 km s^{-1}) followed by Mesozoic sediments above the basement (5.8–6.1 km s^{-1}). Using the lower bound velocity (3.2 km s^{-1}), sediment thickness varies between 800 and 1500 m. Based on upper bound velocity (4.3 km s^{-1}), we find both the sediment thickness and basement depth increase by 600–700 m. The thickness of sediments is more in the northwest and decreases gradually in the southeast, suggesting that the northwestern part of the profile is an important zone for hydrocarbon exploration in the Saurashtra peninsula. With the lower bound velocity of Mesozoics, we find that the basement (5.8–6.1 km s^{-1}) is deep (~2100 m) in the northwest and shallows up near Atkot to ~1.0 km depth, and then deepens further southeast, showing the basement upwarped. The overall velocity and boundary uncertainties are of the order of ±0.15 km s^{-1} and ± 0.15 km respectively.

Keywords: Seismic refraction, sediment thickness, travel-time inversion, volcanic traps.

THE Saurashtra peninsula is almost entirely covered by Deccan volcanics (Traps) with Lower Cretaceous (Mesozoic) sediments exposed in the northeastern part (Figure 1). Significant amount of Mesozoic sediments is believed to be hidden underneath the Deccan Traps. Oil industry has been engaged in exploring trap-covered regions for hydrocarbon potential, since Mesozoic sediments are the source rock for more than 50% hydrocarbon reserves world over[1]. In India, hydrocarbons have been discovered in Mesozoic sediments[2] in Jaisalmer basin of Rajasthan and East Godavari sub-basin of Andhra Pradesh. Presence of subtrappean Mesozoic sediments has been established through geophysical studies and drilling few bore wells in

*For correspondence. (e-mail: asnngri@gmail.com)

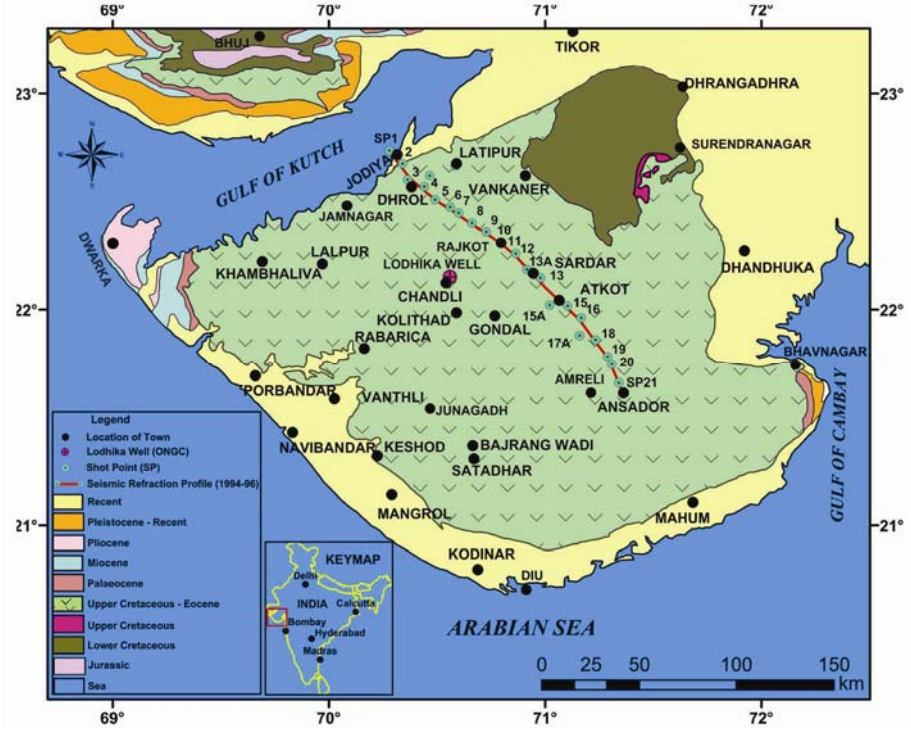

Figure 1. Location of seismic refraction profile along Jodia–Ansador (NW–SE) (modified from ref. 6) shown on geological map of the Saurashtra peninsula, India.

Saurashtra (Lodhika-I, Dhanduka) and adjoining Kutch and Cambay basins[3–8].

Structural imaging in Trap-covered regions is a complex geophysical problem. Near-vertical seismic reflection studies have not been successful in trap-covered regions due to the combined effect of multiple generation, mode conversion, scattering and absorption leading to poor signal-to-noise ratios beneath and within the trap rocks[9,10]. Subtrappean sediments form a low velocity zone (LVZ) in seismic exploration due to the fact that the Trap layer has higher seismic velocity than the velocity of underlying sediments. Seismic refraction studies with large energy sources can provide high-amplitude reflections from subtrappean interfaces at wide-angle range, where the noise is less dominant[7,10]. In certain geological situations such as in regions with thin Trap lying over thick low-velocity sediments, distinct amplitude decay and time 'skip' in first-arrival refraction phases are observed. These signatures are indicative of the presence of low-velocity sediments below high-velocity Trap rocks[11–17]. Therefore, seismic refraction and wide-angle reflection datasets can be effectively used to build a well-constrained subsurface velocity structure in Trap-covered regions.

Oil India Development Board (OIDB) and Oil & Natural Gas Corporation (ONGC) Ltd have sponsored integrated geophysical studies for exploration of subtrappean Mesozoic sediments in Saurashtra peninsula[6]. Seismic refraction studies were carried out along five profiles in Saurashtra peninsula during 1994–96. Here, we present results of seismic refraction data associated with 21 shot points along the Jodia–Ansador profile (Figure 1), with the aim of delineating possible occurrence of subtrappean sediments. The initial model, which was prepared by juxtaposing the 1D velocity–depth functions, obtained by interpretation of first-arrival data[18], was modified by 2D travel-time modelling[19]. The velocity and thickness variation of the Trap and subtrappean sediments, and basement configuration have been determined in the present study.

Seismic data were acquired along the 180 km long Jodia–Ansador profile using two 60-channel DFS-V units from 21 shot points (SP), designated as SP 1 to 21 (Figure 1) by the Controlled Source Seismology Group, National Geophysical Research Institute, Hyderabad during 1994–96. The data were acquired with ~8–10 km shot and 100 m receiver interval on a spread length of 11.8 km recording simultaneously in the form of (a) photographic paper and (b) digital (multiplexed; SEG-B format) magnetic tapes with a 4 ms sampling interval. To enhance the signal strength, six geophones of natural frequency 4.5 Hz were connected in series and bundled at each receiver position. The data were sorted and then used to generate trace normalized record sections for various shot points utilizing the Geomaster Seismic Processing package on CYBER 180/850A mainframe computer. The preliminary processing includes demultiplexing, trace editing, merging and frequency filtering. The record section

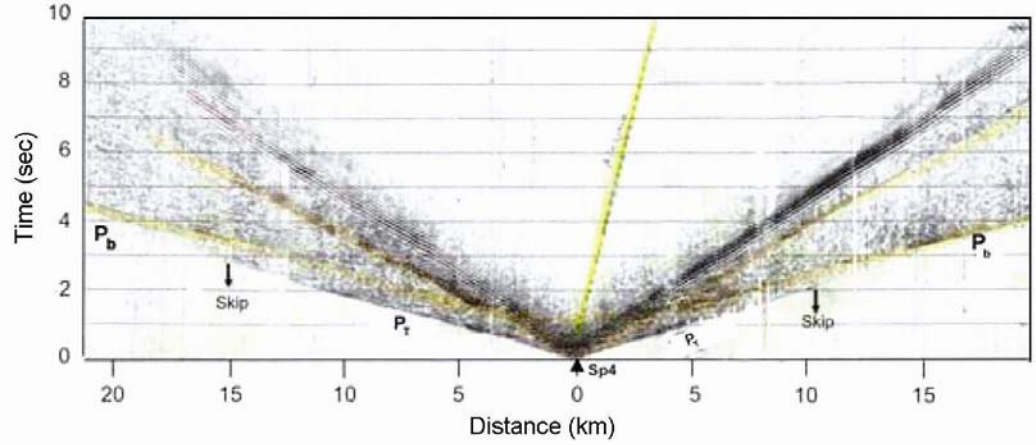

Figure 2. Record section of a typical shot point along the Jodia–Ansador profile. P_T and P_b are first arrival refracted phases through the Deccan Traps and granitic basement respectively. The amplitude decay in P_T and the time 'skip' between P_T and P_b indicate the presence of low-velocity subtrappean sediments in the region.

of SP 4 along the profile has been displayed in Figure 2, as an example.

Interpretation of seismic data generally consists of identification of seismic phases, iterative forward modelling of travel times and inversion. The entire profile is laid on Deccan Trap exposures. Based on change in slope of time–distance first arrivals, two refraction phases (P_T and P_b) are identified (Figure 2). The direct wave recorded with a *P*-wave velocity of 4.9 km s^{-1} represents the Deccan Trap formation all along the profile. The second refracted phase with a *P*-wave velocity of 5.9 km s^{-1} corresponds to the granitic basement, as the velocity (5.7–6.1 km s^{-1}) is characteristic of basement in this region[20]. Record sections of various shot points show decay of P_T amplitudes with increasing offsets. Also, a time 'skip', observed between P_T and P_b indicates the LVZ sandwiched between high-velocity Trap rock and the basement. This might be responsible for decay of energy to the overlying high-velocity layer and delay in arrival time of refraction phase from the deeper high-velocity layer[21]. An increase/decrease in the magnitude of time 'skip' depends on relative thickness of the LVZ. The surface exposure of Cretaceous sediments in the northeastern part of Saurashtra peninsula near the present profile indicates that the sediments may be present below the Deccan Traps, and thus the LVZ may correspond to Mesozoic sediments. The velocity of Mesozoic sediments shows wide variation in this region. Few shot points situated on the exposed Lower Cretaceous (Mesozoic) sediments show the direct-wave velocity of 3.2 km s^{-1}. ONGC Ltd has an exploratory well drilled at Lodhika, west of the present profile. The seismic refraction data along a profile across the well at Lodhika was modelled[22] using the *P*-wave velocity of 3.4–3.6 km s^{-1} for Mesozoic sediments. We find that this sediment thickness does not match with the sediment thickness in the lithologs. From the travel-time inversion of both refraction and wide-angle data along the same profile, the *P*-wave velocity of 4.3 km s^{-1} has been reported for Mesozoic sediments[7]. The deep seismic sounding study along Navibandar–Amreli profile[20] located in the south determined the *P*-wave velocity of 4.0 km s^{-1} for subtrappean Mesozoic sediments. Here, we have modelled the seismic data along Jodia–Ansador profile using both lower (3.2 km s^{-1}) and upper (4.3 km s^{-1}) bound velocities for the low-velocity Mesozoic sediments.

As can be seen from Figure 2, the first-arrival refracted phase (P_T) representing the Deccan Trap terminates and then the first arrival (P_b) representing the basement gets delayed at greater offsets. The Trap direct-wave termination occurs when the wave feels the base of the Trap, consistent with Snell's law, and is refracted into the subtrappean LVZ. The offset at which the direct-wave termination occurs is a function of the velocity structure and thickness of the Trap layer. The Trap thickness will be obtained from the maximum depth penetration of the diving wave that fits the termination point of the Trap diving wave[12]. Similarly, the sediment–basement interface will be constrained using the correct arrival time evident at large shot-receiver offset[10,12].

We derive shallow velocity structure using travel-time inversion of first-arrival seismic data[19], which are picked from the original monitor paper records and assigned uncertainties depending on the offset and signal-to-noise ratio. The reciprocal times for every pair of shot points are checked. There is clear indication of relatively sudden termination in the Trap diving wave (P_T) on the record sections (Figure 2). The offset at which the termination occurs varies substantially from one shot point to the other. For the remainder of this communication, 'offset' will refer to the distance between shot and receiver and 'distance' will refer to profile distance relative to SP 1 at 0 km. Considering the nearby 'Lodhika' well data, geologic/tectonic nature of the region and from the present

data analysis, a LVZ related to subtrappean Mesozoic sediments has been assumed in the study region. While modelling the refraction data, we have considered the *P*-wave velocities of 3.2 and 4.3 km s^{-1} for the LVZ, as we observe them at surface and subsurface respectively. The initial model for 2D travel-time inversion is obtained by merging individual velocity–depth functions for various shot points[18]. The travel times of the first segments (P_T) of each shot point (SP 1 to SP 21) at their respective distances along the profile were inverted simultaneously. This helps determine the velocity variation of the first layer. To find out the thickness of the first layer (Trap), it is important to pick precisely the diving wave (P_T) termination point. After the termination points were picked for all the shot points, rays were traced from individual shot points to their respective termination points, and the base of the Trap layer was determined from the maximum depth penetrated by these rays. Thus the depth of Trap layer which also becomes the top of the LVZ has been obtained (0.2–1.4 km) mainly by modelling the refraction (P_T) data and a few reflection data (P^T) from the bottom of Trap. After the Trap velocity and thickness were determined, we carried out a simultaneous inversion for the basement velocity and sediment–basement interface assuming a velocity of 3.2 and 4.3 km s^{-1} respectively, for the LVZ using the refraction (P_b) data and a few reflection data (P^b) from the basement. Assuming 3.2 km s^{-1} velocity for the LVZ, the basement velocity (5.8–6.1 km s^{-1}) and depth (1.0–2.1 km) variation were obtained. To estimate the possible variation of the basement depth and thereby subtrappean sediment thickness, we have also modelled the data with a velocity of 4.3 km s^{-1} for the LVZ, keeping all other parameters same in the previous modelling. It was observed that both the basement depth and sediment thickness increased by 600–700 m in the northwestern part of the profile up to Atkot.

For the inversion, we have used overall damping factor of 1.0 and have adopted velocity uncertainty of 0.1 km s^{-1} and boundary uncertainty of 0.1 km (refs 14–16, 23), based on a priori estimation[19]. The rays traced through the final velocity model and their travel-time fit are shown for individual (Figure 3) as well as all the shot points together in Figures 4 *a* and 5 *a* assuming 3.2 and 4.3 km s^{-1} for LVZ respectively. Table 1 shows the number of rays traced through the final model, root mean square travel time residual and normalized χ^2 values for various phases corresponding to all shot points. Figures 4 *b* and 5 *b* display the final velocity models corresponding to 3.2 and 4.3 km s^{-1} for LVZ. The velocity model is derived based on the ability to trace rays through the final model to almost all observation points and a trade-off between achieving a sufficiently small travel-time residual of the order of data uncertainties and an adequately high-parameter resolution.

One important aspect of model assessment is to provide a measure of statistical resolution and uncertainty of the estimated model parameters from the diagonal elements of the resolution and covariance matrices respectively. We have carried out resolution and uncertainty tests for the model with LVZ of 3.2 km s^{-1}. Generally, resolution values range from 0 to 1, and depend on the relative number of rays sampling each model parameter. The desired fit and resolution are attained within 3–4 iterations with velocity and boundary resolution >0.9 (Table 2), indicating that the model is well resolved. For obtaining absolute uncertainty of a model parameter, we perturb its value from that in the final model and hold it fixed while inverting the observed data involving all other model parameters that were determined along with the perturbed parameter in the final model[19,24]. Increase or decrease in perturbation is continued until the final model fits the observed data. The maximum perturbation of the parameter that allows a comparable fit to the observed data provides an estimate of its absolute uncertainty. Figure 6 displays the absolute uncertainty of velocity (5.85 km s^{-1}) node and boundary depth (1.9 km) of the basement at 50 km profile distance. This shows the absolute velocity uncertainty lying between 5.73 and 6.0 km s^{-1}, and depth uncertainty between 1.76 and

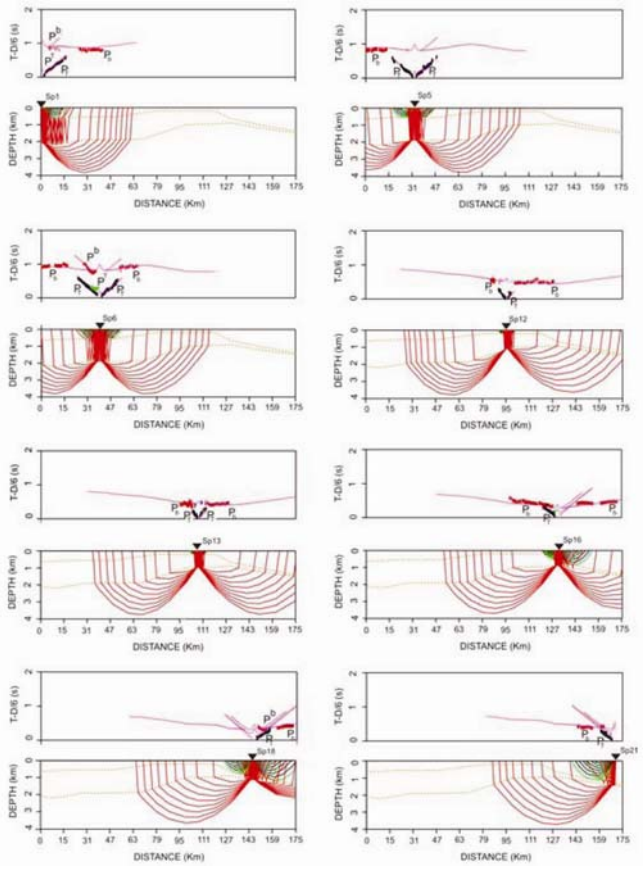

Figure 3. Comparison of observed (vertical bars) and theoretical travel times (line) for various phases (top) and refraction and reflection rays through the final velocity model (with LVZ 3.2 km s^{-1}) (bottom) corresponding to different shot points along the profile.

Table 1. *P*-wave modelling results along the profile

Phase	No. of observations picked	Data uncertainty (ms)	RMS residual (s)	Normalize χ^2 value	No. of rays traced through the model
P_T	1345	60	0.055	0.849	1337
P_b	880	60	0.054	1.870	876
P_T	60	60	0.088	2.829	51
P^b	65	60	0.128	1.750	58

Number of data points used: 2332. RMS travel-time residual: 0.058. Normalized chi-squared: 1.359.

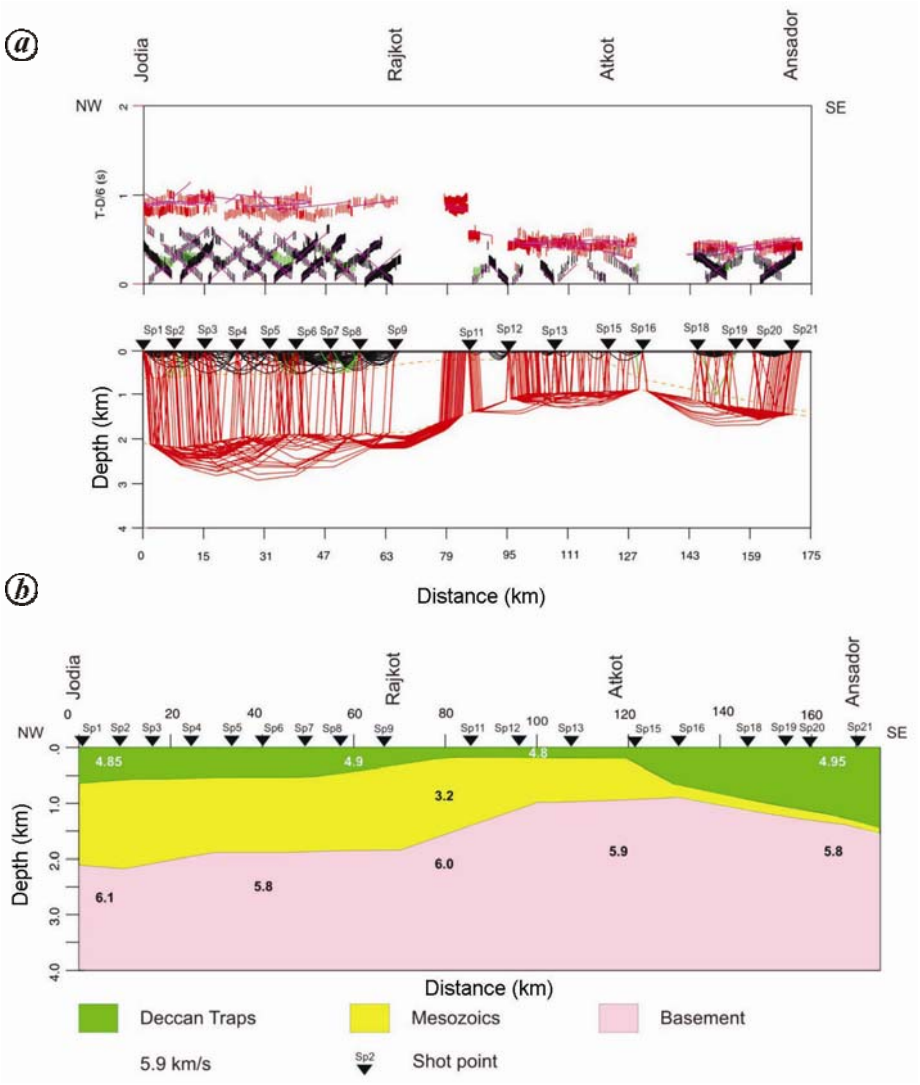

Figure 4. ***a***, Refraction and reflection rays (bottom) traced through the final velocity model (with LVZ 3.2 km s^{-1}) for all the shot points along the profile. Comparison of observed (vertical bars) and theoretical travel times (line) for various phases (top). ***b***, *P*-wave velocity model (LVZ 3.2 km s^{-1}) along the Jodia–Ansador profile. The numbers within the model represent velocities (km s^{-1}) of various layers. Inverted triangles at top show the location of shot points.

2.05 km corresponding to 60 ms travel-time residual. We have carried out the uncertainty test at a few more velocity and boundary nodes and observed that the overall velocity and boundary uncertainties are of the order of ±0.15 km s^{-1} and ±0.15 km respectively.

The velocity model (Figure 4 *b*), derived mainly from the analysis of first-arrival refraction and a few reflection data, reveals the subsurface shallow velocity structure of the Deccan Trap formation, thickness variation of Mesozoic sediments and basement configuration along the

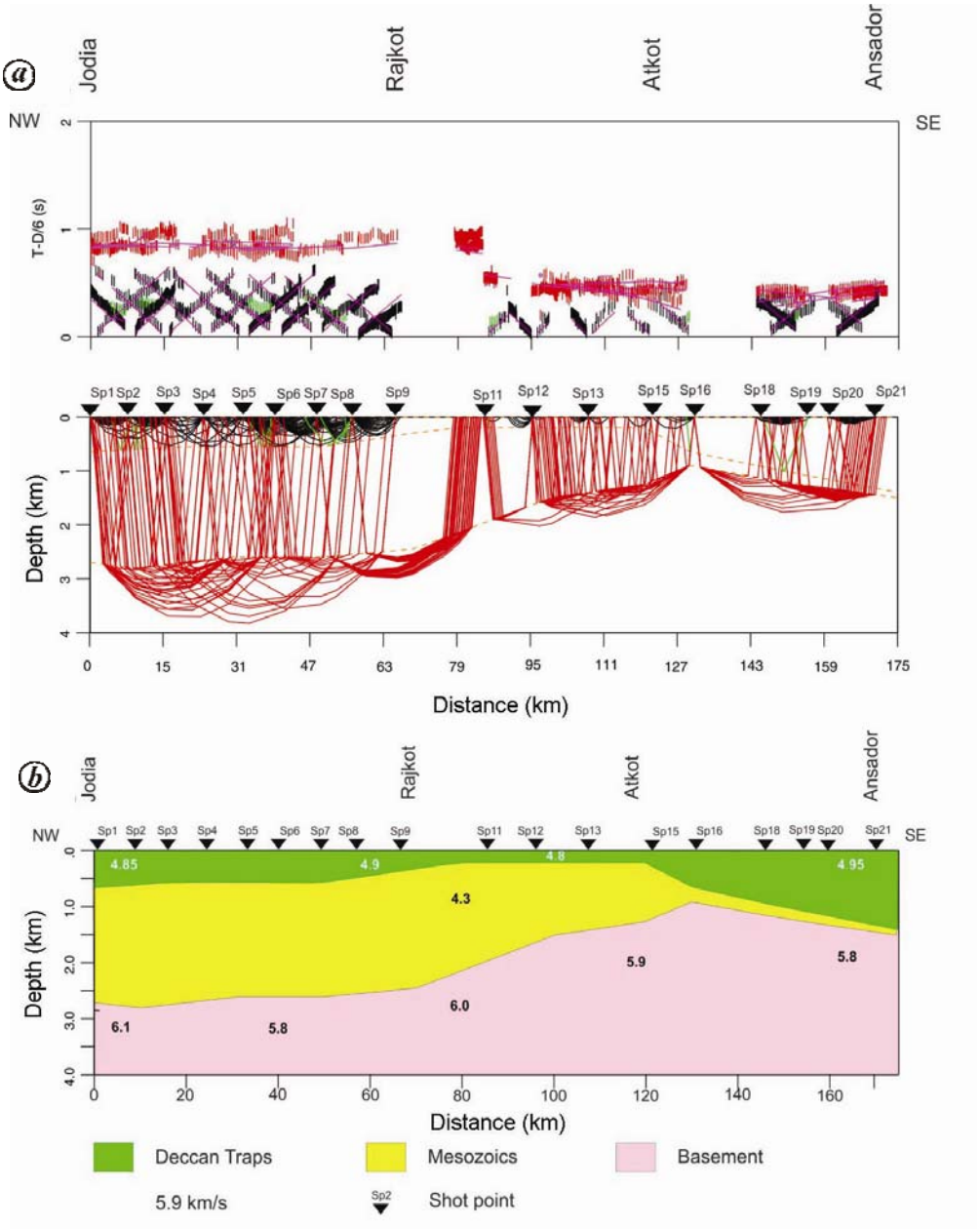

Figure 5. ***a***, Refraction and reflection rays (bottom) traced through the final velocity model (with LVZ 4.3 km s^{-1}) for all the shot points along the profile. Comparison of observed (vertical bars) and theoretical travel times (line) for various phases (top). ***b***, The *P*-wave velocity model (LVZ 4.3 km s^{-1}) along the Jodia–Ansador profile. The numbers within the model represent velocities (km s^{-1}) of various layers. Inverted triangles at the top show the location of shot points.

Jodia–Ansador profile in Saurashtra peninsula. The Trap thickness is about 550–650 m between SP 1 and SP 8, gradually becomes thinner from SP 8 to 80 km profile distance, remains constant up to 120 km and then gradually increases attaining a thickness of about 1400 m near SP 21 at Ansador in the southeast. The second layer corresponds to Mesozoic sediments beneath the Traps, presence of which is indicated by amplitude decay and time 'skip' in the first arrivals. The subtrappean sediments are about 1500 m thick near SP 1 at Jodia in the northwest. The sediment thickness gradually decreases towards southeast up to a profile distance of 120 km. Record sections of SP 16 to SP 21 do not show any amplitude decay or time 'skip' in the first arrivals, indicating that the sediments are almost absent or very thin from SP 16 to further southeast. However, we have modelled a thin subtrappean sedimentary layer between the Trap and the basement. The basement is deep (~2100 m) in the northwest near Jodia, shallow (<1000 m) near Atkot and deepens further southeastward.

Table 2. Resolution estimates along the profile

Distance (km)	Depth nodes (km)	Depth resolution	Standard deviation
0.0	0.65	0.99	0.103
20.0	0.55	0.99	0.081
50.0	0.55	0.98	0.114
70.0	0.30	0.96	0.204
80.0	0.20	0.97	0.172
120.0	0.20	0.81	0.437
130.0	0.65	0.98	0.130
150.0	1.00	0.97	0.185
0.0	2.10	0.98	0.116
10.0	2.20	0.99	0.082
50.0	1.90	0.99	0.068
100.0	1.00	0.98	0.144
120.0	0.95	0.93	0.254
150.0	1.20	0.98	0.130
Distance (km)	**Velocity nodes (km/s)**	**Velocity resolution**	**Standard deviation**
0.0	4.85	1.00	0.001
40.0	4.85	1.00	0.003
60.0	4.90	1.00	0.005
150.0	4.95	0.99	0.005
175.0	4.95	0.93	0.027
10.0	6.00	0.94	0.024
50.0	5.85	0.95	0.023
60.0	5.80	0.92	0.027
80.0	6.00	0.89	0.032
130.0	5.90	0.92	0.028
150.0	5.80	0.97	0.018
175.0	5.80	0.76	0.050

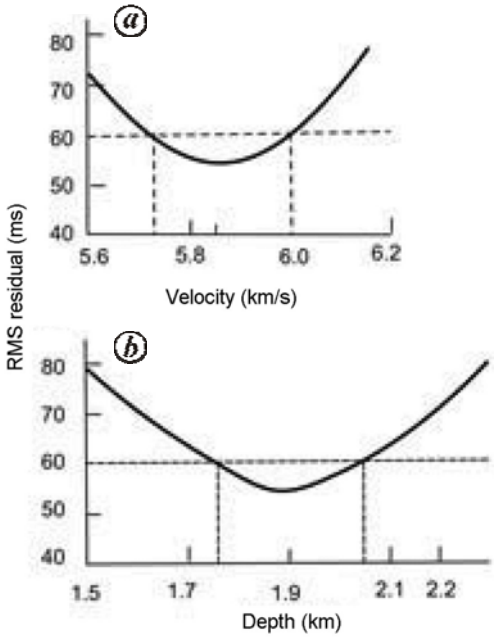

Figure 6. (***a***) Root mean square (rms) travel-time residual as a function of velocity perturbation for the velocity node and (***b***) depth uncertainty for a depth node at 50 km profile distance. The absolute velocity uncertainty lies between 5.73 and 6.0 km s^{-1} (–0.12 to +0.15 km s^{-1}) and depth uncertainty between 1.76 and 2.05 km (–0.14 to +0.15 km) respectively, corresponding to 60 ms travel-time residual.

The modelling result of seismic refraction data along a profile across the well at Lodhika shows a five-layer velocity structure[22]. The trap thickness is about 1350–1500 m and Mesozoic sediment thickness is 1000 m near the well. Whereas the result of inversion along the same profile[7] shows trap (5.05–5.1 km s^{-1}) thickness of about 1.4 km underlain by Mesozoic sediments with thickness varying from 0.9 to 1.6 km. Velocities of the trap and LVZ control the thickness of the trap and Mesozoic layers. Integrated studies[6] along the Jodia–Ansador profile indicate variation of basement depth from 800 to 2000 m and Mesozoic sediment thickness from 200 to 1300 m. Gravity studies along the Jodia–Ansador profile indicate high-density intrusive in the basement for gravity high in the residual gravity field south of Jodia. Joint inversion of magnetotelluric and deep resistivity sounding results show about 1000 m thickness of Deccan Traps and about 1000 m thick Mesozoic sediments below the traps. The sediment thickness reduces from Jodia towards Ansador, and the basement is upwarped near Atkot. The deep resistivity studies indicate increase of trap layer thickness towards Ansador and sediment thickness of about 1500 m towards Rajkot. The basement is upwarped with a depth of about 1000 m near Atkot and deepening on either side.

The model derived in this study suggests basement upwarp southeast of Rajkot and a different subsurface structure southeast and northwest of Rajkot. This can be attributed to the upwelling introduced by volcanic plug/dyke that might have produced diffractions observed on seismic records[6]. The thick Trap near Ansador has a major problem for the identification of any signature of sub-trappean sediments in the southeastern part of the profile.

The presence of Mesozoic sediments below the Deccan Traps in Saurashtra peninsula has been indicated by amplitude decay and travel time 'skip' in the refraction data. The present study delineated the subsurface structure of low-velocity Mesozoic sediments below the high-velocity Deccan Traps along Jodia–Ansador profile. The Mesozoic sediments are thick (1500 m) in the northwest near Jodia, and may be absent or very thin southeastward, which indicates that the northwestern part of the Saurashtra peninsula may form an important zone for detailed investigation of hydrocarbons. The velocity of Trap layer varies from 4.8 to 5.0 km s^{-1} and thickness is about 1400 m near Ansador in the southeast. The basement (5.8–6.1 km s^{-1}) is deep near Jodia in the northwest.

1. Bois, C., Bouche, P. and Pelet, R., Global geological history and distribution of hydrocarbon reserves. *AAPG Bull.*, 1982, **66**, 1248–1270.
2. Mayor, S., Sawkar, S. S., Gangaram, Das, A. K. and Painuly, S. P., An integrated approach to the Mesozoic exploration in Rajpardi area, South Cambay basin, Gujarat, India. In 4th International Conference and Exposition on Petroleum Geophysics, Society of Petroleum Geophysicists, Mumbai, 2002.

3. Roy, T. K., Structural styles in southern Cambay basin, India and role of Narmada geofracture in formation of giant hydrocarbon accumulation. *Bull. ONGC*, 1991, **27**, 15–56.
4. Prasad, B. N., Khan, S. and Giridhar Lal., Hydrocarbon prospects of Kutch basin onland, India. *J. Assoc. Explor. Geophys*., 1994, **15**(4), 161–169.
5. Singh, D., Alat, C. A., Singh, R. N. and Gupta, V. P., Source rock characteristics and hydrocarbon generating potential of Mesozoic sediments in Lodhika area, Saurashtra basin, Gujarat, India. In Proceedings Second International Petroleum Conference and Exhibition PETROTECH-97, New Delhi, 1997, pp. 205–220.
6. NGRI, Integrated geophysical studies for hydrocarbon exploration in Saurashtra, India. NGRI Technical Report No. NGRI-1998-Exp-237, 1998.
7. Sain, K., Zelt, C. A. and Reddy, P. R., Imaging subvolcanic Mesozoics using travel time inversion of wide-angle seismic data in the Saurashtra peninsula of India. *Geophys. J. Int*., 2002, **150**, 820–826.
8. Prasad, A. S. S. S. R. S., Sain, K. and Sen, M. K., Imaging sub basalt Mesozoics along Jakhau–Mandvi and Mandvi–Mundra profiles in Kutch sedimentary basin from seismic and gravity modelling. *Geohorizons*, 2013, **18**(2), 51–56.
9. Dowle, R., Mandroux, F., Soubaras, R. and Williams, G., Uses of wide azimuth and variable-depth streamers for sub-basalt seismic imaging. *First Break*, 2011, **29**(12).
10. Jarchow, C. M., Catchings, R. D. and Lutter, W. J., Large explosive source, wide-recording aperture, seismic profiling on the Columbia Plateau, Washington. *Geophysics*, 1995, **59**, 259–271.
11. Fruehn, J., Fliendner, M. M. and White, R. S., Integrated wide-angle and near-vertical sub salt study using large-aperture seismic data from the Faeroe–Shetland region. *Geophysics*, 2001, **66**(5), 1340–1348.
12. Tewari, H. C., Dixit, M. M. and Murty, P. R. K., Use of travel time skips in refraction analysis to delineate velocity inversion. *Geophys. Prospect*., 1995, **43**, 793–804.
13. Sain, K. and Kaila, K. L., Ambiguity in the solution of the velocity inversion problem and a solution by joint inversion of seismic refraction and wide-angle reflection times. *Geophys. J. Int.*, 1996, **124**, 215–227.
14. Murty, A. S. N., Prasad, B. R., Koteswara Rao, P., Raju, S. and Sateesh, T., Delineation of Subtrappean Mesozoic sediments in Deccan Syneclise, India, using travel time inversion of seismic refraction and wide-angle reflection data. *PAGEOPH*, 2010, **167**, 233–251.
15. Murty, A. S. N., Dixit, M. M., Mandal, B., Raju, S., Sanjaykumar, Karupanan, P., Anitha, K. and Sarkar, D., Extension of Godavari Gondwana sediments underneath Trap covered region of Satpura basin as evidenced from seismic studies in Deccan syneclise, India. *J. Asian Earth Sci.*, 2011, **42**(6), 1232–1242.
16. Murty, A. S. N., Koteswara Rao, P., Dixit, M. M., Kesava Rao, G., Reddy, M. S., Prasad, B. R. and Sarkar, D., Basement configuration of the Jhagadia–Rajpipla profile in the western part of Deccan syneclise, India from travel-time inversion of seismic refraction and wide-angle reflection data. *J. Asian Earth Sci.*, 2011, **40**, 40–51.
17. Sain, K., Reddy, P. R. and Behera, L., Imaging of low-velocity Gondwana sediments in the Mahanadi delta of India using travel time inversion of first arrival seismic data. *J. Appl. Geophys*., 2002, **49**, 163–171.
18. Sain, K. and Kaila, K. L., Interpretation of first arrival times in seismic refraction work. *Pure Appl. Geophys*., 1996, **147**, 181–194.
19. Zelt, C. A. and Smith, R. B., Seismic travel time inversion for 2-D crustal velocity structure. *Geophys. J. Int*., 1992, **108**, 16–34.
20. Kaila, K. L., Tewari, H. C. and Sarma, P. L. N., Crustal structure from deep seismic studies along Navibandar–Amreli profile in Saurashtra. *Indian Mem. Geol. Soc. India*, 1980, **3**, 218–232.
21. Greenhalgh, S. A., Comments on 'The hidden layer problem in seismic refraction work'. *Geophys. Prospect.*, 1977, **25**, 179–181.
22. Dixit, M. M., Satyavani, N., Sarkar, D., Khare, P. and Reddy, P. R., Velocity inversion in the Lodhika area, Saurashtra peninsuls, Western India. *First Break*, 2000, **18**, 12.
23. Murty, A. S. N., Sain, K. and Rajendra Prasad, B., Velocity structure of the West-Bengal sedimentary basin, India along the Palashi–Kandi profile using travel time inversion of wide-angle seismic data and gravity modelling-an update. *PAGEOPH*, 2008, **165**, 1733–1750.
24. Zelt, C. A., Modeling strategies and model assessment for wide-angle seismic travel time data. *Geophys. J. Int*., 1999, **139**, 183–204.

ACKNOWLEDGEMENTS. We thank the Director, CSIR-NGRI, Hyderabad for permission to publish this work and members of the CSS field party for recording seismic data, and Mr V. Rajasekhar and Mr Satendra Singh for preparing the figures. We also thank Prof. Saibal Gupta (IIT Kharagpur) and two other anonymous reviewers for constructive suggestions that have helped to improve the manuscript. This is a contribution to SHORE project under the 12th Five Year Scientific Programme of CSIR-NGRI.

Received 3 June 2015; revised accepted 31 December 2015

doi: 10.18520/cs/v110/i9/1844-1851